⌘ *Author's Choice*

THE JOURNAL OF BIOLOGICAL CHEMISTRY VOL. 288, NO. 3, pp. 1428–1438, January 18, 2013


# Glycosylation-independent Lysosomal Targeting of Acid α-Glucosidase Enhances Muscle Glycogen Clearance in Pompe Mice*

Received for publication, November 20, 2012 Published, JBC Papers in Press, November 27, 2012, DOI 10.1074/jbc.M112.438663

**John A. Maga[‡1], Jianghong Zhou[‡2], Ravi Kambampati[‡1], Susan Peng[‡], Xu Wang[§], Richard N. Bohnsack[¶], Angela Thomm[‡3], Sarah Golata[‡4], Peggy Tom[‡5], Nancy M. Dahms[¶], Barry J. Byrne[§], and Jonathan H. LeBowitz[‡6]**

*From [‡]ZyStor Therapeutics, Milwaukee, Wisconsin 53226-4838, the [§]Powell Gene Therapy Center, College of Medicine, University of Florida, Gainesville, Florida 32610-0266, and the [¶]Department of Biochemistry, Medical College of Wisconsin, Milwaukee, Wisconsin 53226-4801*

**Background:** Acid α-glucosidase, an enzyme replacement therapy for Pompe disease, is poorly targeted to lysosomes when relying on phosphomannose residues.
**Results:** Fusing IGF-II to acid α-glucosidase resulted in more efficient uptake and glycogen clearance from muscle of Pompe mice.
**Conclusion:** Enhanced binding to the cation-independent mannose 6-phosphate receptor (CI-MPR) enabled improved glycogen clearance in Pompe mice.
**Significance:** BMN 701 is now being tested for Pompe disease in human clinical studies.

**We have used a peptide-based targeting system to improve lysosomal delivery of acid α-glucosidase (GAA), the enzyme deficient in patients with Pompe disease. Human GAA was fused to the glycosylation-independent lysosomal targeting (GILT) tag, which contains a portion of insulin-like growth factor II, to create an active, chimeric enzyme with high affinity for the cation-independent mannose 6-phosphate receptor. GILT-tagged GAA was taken up by L6 myoblasts about 25-fold more efficiently than was recombinant human GAA (rhGAA). Once delivered to the lysosome, the mature form of GILT-tagged GAA was indistinguishable from rhGAA and persisted with a half-life indistinguishable from rhGAA. GILT-tagged GAA was significantly more effective than rhGAA in clearing glycogen from numerous skeletal muscle tissues in the Pompe mouse model. The GILT-tagged GAA enzyme may provide an improved enzyme replacement therapy for Pompe disease patients.**

Pompe disease is a lysosomal storage disorder caused by insufficient lysosomal acid α-glucosidase (GAA)[7] activity (1–3). GAA hydrolyzes the α-1,4 and α-1,6 linkages in branched glycogen molecules (4). GAA deficiency results in the accumulation of excess glycogen primarily in the lysosomes of skeletal and cardiac muscle, leading to progressive muscle weakness and cardiorespiratory failure. There is a broad spectrum in the severity and age of onset of Pompe disease that roughly correlates with the residual amount of GAA activity present in patient tissues (5). The severe infant-onset Pompe disease is characterized by hypertropic cardiomyopathy, respiratory insufficiency, and general muscle weakness with death usually resulting by 1 year of age when untreated (6). Late-onset Pompe disease is characterized by progressive muscle weakening with respiratory failure the most common cause of death (7).

Currently, enzyme replacement therapy using alglucosidase alfa, recombinant human GAA (rhGAA) produced in Chinese hamster ovary (CHO) cells is an approved treatment for patients with Pompe disease. Generally, the clinical experience with alglucosidase alfa suggests that enzyme replacement therapy is more effective in addressing the cardiomyopathy in infant-onset patients and less effective in treating the cellular pathology of skeletal muscle in infant- and late-onset patients (6, 8–11).

In the Pompe mouse knock-out model (12), glycogen is also cleared from heart tissue more readily than from skeletal muscle (13–15). In fact, rhGAA doses of 100 mg/kg weekly were required to achieve maximal clearance of glycogen from skeletal muscle, and treatment of Pompe mice with multiple weekly doses of 20 mg/kg rhGAA cleared only between 0 and 40% of glycogen from quadriceps.

The marketed dose of alglucosidase alfa (20 mg/kg biweekly) is relatively high compared with the dose of approved therapeutics for other lysosomal storage diseases (biweekly doses between 0.5 and 1 mg/kg for Gaucher, Fabry, and mucopolysaccharidosis I), suggesting that delivery of rhGAA to the lysosome of skeletal muscle is of limited efficiency. In part, this is because of the intrinsic properties of skeletal muscle, such as the low

* This work was supported by ZyStor Therapeutics, Inc. (now BioMarin Pharmaceuticals Inc.).
⌘ *Author's Choice*—Final version full access.
[1] Present address: BioMarin Pharmaceutical, Inc., 105 Digital Dr., Novato, CA 94949.
[2] Present address: Oncode-Med Inc., Basking Ridge, NJ 07920.
[3] Present address: PhysioGenix, Inc., Milwaukee, WI 53226.
[4] Present address: Benz Oil, Milwaukee, WI 53209.
[5] Present address: Cytometix, Milwaukee, WI 53226.
[6] To whom correspondence should be addressed: BioMarin Pharmaceutical, Inc., 105 Digital Dr., Novato, CA 94949. Tel.: 415-506-6850; Fax: 415-382-7427; E-mail: jlebowitz@bmrn.com.
[7] The abbreviations used are: GAA, acid α-glucosidase; M6P, mannose 6-phosphate; IGF-II, insulin-like growth factor II; GILT, glycosylation-independent lysosomal targeting; DPBS, Dulbecco's phosphate-buffered saline; rhGAA, recombinant human GAA; PNP, *para*-nitrophenol; CI-MPR, cation-independent mannose 6-phosphate receptor; BisTris, 2-[bis(2-hydroxyethyl)amino]-2-(hydroxymethyl)propane-1,3-diol; RU, resonance units.

abundance of the cation-independent mannose 6-phosphate receptor (CI-MPR), altered lysosomal function leading to increased autophagy particularly in type II muscle fibers (19, 20), and the relatively low blood flow to skeletal muscle tissue compared with liver, heart, and other tissues. However, the problem is exacerbated by the low affinity of CHO-produced rhGAA for the CI-MPR, which results in diminished lysosomal targeting from the extracelluar pathway (3, 21, 22).

rhGAA is delivered to the lysosome by receptor-mediated endocytosis after binding of bis-mannose 6-phosphorylated glycan (bis-M6P-glycan) on the rhGAA protein surface to the CI-MPR. rhGAA has only about 0.9–1.2 mol M6P/mol enzyme, and only a small fraction of rhGAA oligosaccharides have bis-M6P (14, 15). As oligosaccharides with only a single M6P bind to the CI-MPR with a 1000-fold lower affinity (24), rhGAA preparations are not efficiently targeted to the lysosome.

Delivery of rhGAA can be improved by providing high affinity ligands for the CI-MPR. One approach used was the conjugation of bis-M6P-containing oligosaccharides to rhGAA. This neo-rhGAA displayed an increase in cellular uptake *in vitro* and *in vivo* and an increase in glycogen clearance from Pompe mouse muscle tissue (14, 25).

We have used a peptide-based, glycosylation-independent lysosomal targeting (GILT) approach to create an rhGAA molecule containing a high affinity ligand for the CI-MPR. Previously, fusion of a portion of human IGF-II to the human lysosomal enzyme β-glucuronidase, deficient in mucopolysaccharidosis VII (MPS VII), was shown to promote efficient uptake into cultured MPS VII fibroblasts and delivery of active enzyme to a wide range of cell types in MPS VII mice through binding of the IGF-II-derived GILT tag to the CI-MPR (26).

We fused the GILT tag to the N terminus of rhGAA to create a GAA enzyme (BMN 701) with high affinity for the CI-MPR receptor. BMN 701 has biochemical properties similar to those of rhGAA but is delivered more effectively to the lysosomes of L6 myoblasts *in vitro*. Administration of GILT-tagged BMN 701 to Pompe model mice greatly increases the clearance of accumulated glycogen in muscle tissue compared with equivalent doses of rhGAA. Use of the GILT peptide tag addresses the relatively ineffective targeting of rhGAA caused by poor M6P phosphorylation, and the BMN 701 molecule is now being tested in a phase I-II clinical study to determine whether its increased efficiency of targeting will improve clinical outcomes.

## EXPERIMENTAL PROCEDURES

*Plasmids*—DNA cassette 635 encoding complete human GAA amino acids 1–952 was derived from IMAGE clone 4374238 (Open Biosystems) using PCR primers GAA13 (5′-ggaattcCAACCATGGGAGTGAGGCACCCGCCC-3′) and GAA27 (5′-gctctagaCTAACACCAGCTGACGAGAAACTGC-3′). This cassette was digested with EcoRI and XbaI, blunted by treatment with Klenow DNA polymerase, and then ligated into the Klenow-treated HindIII site of expression vector pCEP4 (Invitrogen) to create plasmid p635.

DNA cassette 701 was identical to cassette 635 except for the following GILT tag-containing N-terminal sequence that was joined upstream of GAA amino acid Ala-70: gaattcACACCAATGGGAATCCCAATGGGGAAGTCGATGCTGGTGCTTCTCACCTTCTTGGCCTTCGCCTCGTGCTGCATTGCTGCTCTGTGCGGCGGGGAGCTGGTGGACACCCTCCAGTTCGTCTGTGGGGACCGCGGCTTCTACTTCAGCAGGCCCGCAAGCCGTGTGAGCCGTCGCAGCCGTGGCATCGTTGAGGAGTGCTGTTTCCGCAGCTGTGACCTGGCCCTCCTGGAGACGTACTGTGCTACCCCCGCCAAGTCCGAGggcgcgccg. This cassette was digested with EcoRI and XbaI, blunted by treatment with Klenow DNA polymerase, and then ligated into the Klenow-treated HindIII site of expression vector pCEP4 to create plasmid p701. The 701 cassette encodes the IGF-II signal peptide, residues 1 and 8–67 of mature human IGF-II, a three-amino acid spacer, and residues 70–952 of GAA. For large scale production of GILT-tagged GAA in CHO cells, the coding region of DNA cassette 701 was cloned into the GPEx® retrovector expression system as described (27).

The 5′-end of DNA cassette 1288 (gaattcACACCAATGGGAATCCCAATGGGGAAGTCGATGCTGGTGCTTCTCACCTTCTTGGCCTTCGCCTCGTGCTGCATTGCTGCTggcgcgccgaccggtcaccatcaccatcaccacgcgccgggcctgaacgacatcttcgaggcccagaagatcgagtggcacgaa) encodes the IGF-II signal sequence followed by six histidine residues and a BirA biotinylation acceptor site (see below). This sequence was cloned upstream of the coding region for human CI-MPR domains 10–13 (amino acids P1363–P1988) (28) followed by the sequence TGAGCGGCCGC encoding a stop codon and NotI site. The 5′-end of this cassette was digested with EcoRI and blunted with Klenow DNA polymerase. The 3′-end of the cassette was digested with NotI. The cassette was ligated into vector pCEP4 at the 5′ Klenow-treated HindIII site and 3′ NotI site to create plasmid p1288. Plasmid p1355 was identical to p1288 except that the two codons encoding amino acids 1572–1573 were changed to the sequence ACTAGT to yield the point mutation I1572T and a silent mutation in Ser-1573 that creates a diagnostic SpeI site. All expression cassette sequences were verified by di-deoxy DNA sequencing.

*Tissue Culture*—For many experiments, GILT-tagged GAA and rhGAA were purified from culture supernatants of transiently transfected HEK293 cells. For transient transfections, plasmids p701 and p635 were transfected into suspension FreeStyle 293-F cells as described by the manufacturer (Invitrogen). Briefly, cells were grown in Opti-MEM I medium (Invitrogen) in polycarbonate shaker flasks on an orbital shaker at 37 °C in 8% $CO_2$. Cells were adjusted to a concentration of $1 \times 10^6$ cells/ml and then transfected with a 1:1:1 ratio of ml cells:μg DNA:μl 293Fectin. Cultures were harvested 5–10 days post-transfection and centrifuged at 5,000 × *g* for 20 min. Culture supernatants were filtered through a 0.8/0.2-μm AcroPak 500 capsule (Pall) and concentrated with a tangential flow device with a 30,000 MWCO PLTK filter (Millipore). Sodium acetate, pH 4.6, was added to a final concentration of 0.1 M, and concentrated supernatants were quick-frozen in liquid nitrogen and stored at −80 °C.

A stable cell line suitable for large scale production of the GILT-tagged 701 cassette in CHO cells was generated with the GPEx® retrovector expression system as described (27). The resulting BMN 701 CHO cell line was grown in 5 liters of PF-CHO LS medium (HyClone) in a 10-liter Wave bioreactor at 37 °C in 5% $CO_2$. Cultures were supplemented with R15.4

(HyClone). On day 5 cultures were shifted to 31 °C and then harvested on day 11 and frozen at −80 °C.

L6 rat myoblasts (ATCC, CRL-1458) and C2C12 mouse myoblasts (ATCC, CRL-1772) were grown in DMEM (Invitrogen) supplemented with 10% fetal bovine serum (Invitrogen) in 75-$cm^2$ tissue culture flasks (Corning) at 37 °C and 5% $CO_2$.

*CI-MPR Biotinylation*—Supernatant from FreeStyle 293-F cells transfected with plasmids p1288 and p1355 were applied to a 1-ml His-GraviTrap column (GE Healthcare) as directed by the manufacturer for purification of the $His_6$-tagged receptor domain proteins. Eluted proteins were concentrated, exchanged into 10 mM Tris, pH8, and 25 mM NaCl buffer, and then biotinylated with BirA enzyme as described by the manufacturer (Avidity) in reactions that contained 70 μg of receptor in 205 μl, 10 mM Tris, pH 8, 25 mM NaCl buffer, 25 μl of BiomixA, 25 μl of BiomixB, and 4 μl of BirA enzyme. BirA enzyme treatment was performed at 30 °C for 1.5 h. The reactions were then diluted 20-fold into His GraviTrap binding buffer (GE Healthcare) and reapplied to the His GraviTrap column for removal of BirA enzyme and free biotin. Biotinylated CI-MPR constructs were stored at 4 °C.

*Protein Purification*—Cell culture supernatants adjusted to pH 4.6 with sodium acetate were thawed from storage at −80 °C, and ammonium sulfate was added to 0.75 M. The material was centrifuged to remove precipitation and filtered with a 0.8/0.2-μm AcroPak 500 capsule (Pall). The filtered material was loaded onto a phenyl-Sepharose 6 Fast Flow (low sub) (GE Healthcare) column prepared with HIC load buffer (50 mM sodium acetate, pH 4.6, 0.75 M ammonium sulfate). The column was washed with 10 column volumes of HIC wash buffer (50 mM sodium acetate, pH 5.3, 0.75 M ammonium sulfate) and eluted with 5 column volumes of HIC elution buffer (50 mM sodium acetate, pH 5.3, 20 mM ammonium sulfate). Pooled fractions were dialyzed extensively into QXL load buffer (20 mM histidine, pH 6.5, 50 mM NaCl) and then loaded onto a Q Sepharose XL column (GE Healthcare). The column was washed with 10 column volumes of QXL load buffer and eluted with 10 column volumes of QXL elution buffer (20 mM histidine, pH 6.5, 150 mM NaCl). Purified samples were concentrated by ultrafiltration, and buffer was exchanged into phosphate-buffered saline, pH 6.2. Samples were snap-frozen in liquid nitrogen and stored at −80 °C. Alglucosidase alfa was recovered from excess material of the reconstituted commercial product used in patients.

*Enzyme Assays*—Assay substrates and standards were obtained from Sigma. For GAA *para*-nitrophenol (PNP) assays, enzyme was incubated in 50-μl reactions containing 100 mM sodium acetate, pH 4.2, with 10 mM PNP α-glucoside substrate. Reactions were incubated at 37 °C for 20 min and stopped with 300 μl of 100 mM sodium carbonate. Absorbance at 405 nm was read in 96-well microtiter plates and compared with standard curves derived from *p*-nitrophenol. 1 GAA PNP unit is defined as nmol PNP hydrolyzed/ml enzyme/h. Specific activities were determined by dividing GAA PNP units by the protein concentration as determined by the Bradford assay (Bio-Rad). Saturation curves were generated by incubating 0.5 μg of GAA protein in PNP assays with increasing amounts of PNP α-glucoside ranging from 0 to 20 mM substrate. Plots of product formation *versus* substrate concentration were fit to the Michaelis-Menten equation with KaleidaGraph software (Synergy Software) to determine $K_m$ values.

GAA was also assayed using 4-methylumbelliferyl α-D-glucosidase substrate. The enzyme was incubated in 20-μl reactions containing 123 mM sodium acetate, pH 4.0, with 10 mM 4-methylumbelliferyl α-D-glucosidase substrate. Reactions were incubated at 37 °C for 1 h and stopped with 200 μl of buffer containing 267 mM sodium carbonate and 427 mM glycine, pH 10.7. Fluorescence was read with 355 nm excitation and 460 nm filters in 96-well microtiter plates and compared with standard curves derived from 4-methylumbelliferone. One GAA 4-methylumbelliferyl unit is defined as nmol 4-methylumbelliferone hydrolyzed/ml/h.

*Uptake Assays*—Rat L6 myoblast cells were seeded into 24-well tissue culture plates (Corning), grown for 24 h to ~90% confluency. Cells were washed once with uptake medium (DMEM, high glucose, supplemented with 0.5 g/liter bovine serum albumin (Sigma), 4 mM L-glutamine (Invitrogen), and 20 mM HEPES, pH 7.2), and then incubated at 37 °C and 5% $CO_2$ in uptake medium containing purified rhGAA or BMN 701. Some wells also contained either 5 mM M6P (Calbiochem) or 2.4 mM IGF-II (Cell Sciences) as an inhibitor. After 18 h, cells were washed four times with DPBS, pH 7.4 (0.133 g/liter $CaCl_2 \cdot 2H_2O$, 0.1 g/liter $MgCl_2 \cdot 6H_2O$, 0.2 g/liter KCl, 0.2 g/liter $KH_2PO_4$, 8.0 g/liter NaCl, 1.15 g/liter $Na_2HPO_4$), and then lysed with the addition of 200 μl/well CelLytic M reagent (Sigma) and 20 min of shaking at room temperature. Lysate debris was removed by centrifugation at 2,000 × *g* for 5 min. Lysate GAA activity of duplicate wells was measured with the GAA 4-methylumbelliferyl assay and normalized to lysate protein concentration as determined using the bicinchoninic acid protein assay (Pierce).

*SDS-PAGE, Western Blot Analysis, and Antibodies*—Protein samples were separated on Criterion XT 4–12% BisTris reducing SDS-PAGE (Bio-Rad) at 200 V for 50 min as described by the manufacturer. Silver staining was performed as described (29). For Western blots, samples were transferred to Hybond-P membranes (GE Healthcare) and probed using the ECL system (GE Healthcare) as described by the manufacturer. Dilution of primary anti-GAA mouse monoclonal 3A6-1F2 antibody was 1:100,000. Rabbit polyclonal anti-IGF2 (Cell Sciences, PA0382) and anti-GAA PAb2443 were diluted 1:1000 and 1:200, respectively. Horseradish peroxidase-conjugated secondary anti-mouse IgG and anti-rabbit IgG antibodies (BioChain) were diluted 1:5,000. Molecular weight markers were from Bio-Rad. Anti-GAA monoclonal antibody 3A6-1F12 was generated using rhGAA as antigen, and antibody used in this study was purified from ascites fluid by QED Bioscience. Polyclonal antibody 2443 was produced in rabbits using rhGAA excised from an SDS-polyacrylamide gel as antigen.

*Immunofluorescence*—C2C12 mouse myoblasts were grown on polylysine-coated slides (BD Biosciences) and incubated for 18 h in the presence or absence of 100 nM BMN 701 at 37 °C in 5% $CO_2$. Cells were incubated in growth medium for 1 h and then washed four times with DPBS before fixing with methanol at room temperature for 1 h. The following incubations were all at room temperature, each separated by three washes in DPBS.

Incubations were for 1 h unless noted. Slides were permeabilized with 0.1% Triton X-100 for 15 min and then blocked with blocking buffer (10% heat-inactivated horse serum (Invitrogen) in DPBS). Slides were incubated with primary mouse monoclonal anti-GAA antibody 3A6-1F2 (1:5000 in blocking buffer) and then with secondary rabbit anti-mouse IgG AF594-conjugated antibody (Invitrogen A11032, 1:200 in blocking buffer). A FITC-conjugated rat anti-mouse LAMP-1 (BD Pharmingen 553793, 1:50 in blocking buffer) was then incubated. Slides were mounted with DAPI-containing mounting solution (Invitrogen) and viewed with a Nikon Eclipse 80i microscope equipped with fluorescein isothiocyanate, Texas Red, and DAPI filters (Chroma Technology). Images were captured with a photometric Cascade camera controlled by MetaMorph software (Universal Imaging). Images were merged using Photoshop software (Adobe).

*Surface Plasmon Resonance Analysis*—All surface plasmon resonance measurements were performed at 25 °C using a BIAcore 3000 instrument. SA sensor chips and surfactant P20 were obtained from GE Healthcare. All buffers were filtered using Nalgene filtration units (0.2 μm), equilibrated to room temperature, and degassed immediately prior to use. Protein samples were centrifuged (15 min at 13,000 × *g*) to remove any particulates that might be present in the sample. Purified biotinylated wild-type (1288) or mutant (1355; containing a single amino acid substitution that effectively decreases the affinity of the receptor for IGF-II) CI-MPR constructs were immobilized on separate surfaces on a BIAcore streptavidin SA chip to a final RU of 280 and 300, respectively. IGF-II and BMN 701 proteins were passed over the surfaces at a flow rate of 40 μl/min for 3 min in 50 mM HEPES, pH 7.4, 0.15 M NaCl, and 0.005% (v/v) Surfactant P20. The surfaces were regenerated by a 1-min injection of 10 mM hydrochloric acid at 10 μl/min prior to the next injection of protein.

Proteins were diluted just prior to beginning the concentration curves to minimize the amount of time that the samples were at room temperature. Each concentration was run in duplicate for the individual concentration curves. All response data were double referenced (30), where controls for the contribution of the change in refractive index were performed in parallel with the 1355 protein-coupled flow cell and subtracted from all binding sensorgrams. The concentration curves were analyzed and fit with either the 1:1 Langmuir kinetic model (BIAevaluation software package 4.0.1) or by steady-state kinetics (Sigmaplot). Shown are the results from separate trials of each protein run in duplicate.

*Animal Injections and Measurement of Tissue Glycogen Levels*—The 129-GAA$^{-/-}$ Pompe mouse line used in these experiments was derived from the original Pompe mouse model 6$^{neo}$/6$^{neo}$ strain (12). Animals were tolerized with a 25-μg subcutaneous injection of BMN 701 within 48 h after birth. Five animals in each group (2 months old) were given four weekly injections of either rhGAA or BMN 701 at two dosage levels, 5 and 20 mg/kg. Five untreated animals used as controls received four weekly injections of saline solution. Mice were sacrificed 1 week after the fourth injection, and diaphragm, heart, soleus, quadriceps, gastrocnemius, tibialis anterior, extensor digitorum longus, and tongue tissues were harvested for glycogen level analysis. Of the 40 initial mice (5 animals/group), 8 died during the experiment: 2 control animals, 2 animals from each of the low dose groups (rhGAA and BMN 701, 5 mg/kg), and 1 animal from each high dose group (rhGAA and BMN 701 20 mg/kg). The animals were reared in groups with no evidence of chronic illness. Animals died evenly across all groups, so the animal deaths are not thought to be compound related.

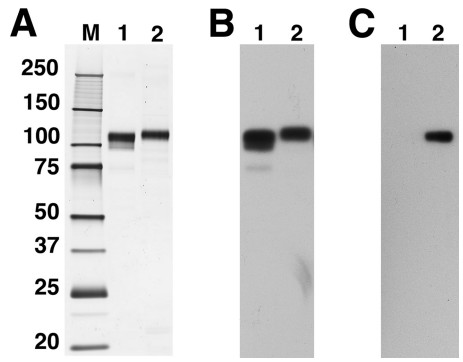


FIGURE 1. **SDS-PAGE and Western blots.** 100 ng of untagged rhGAA and HEK293-produced BMN 701 used in studies in this report (*lanes 1* and *2*, respectively) were separated by reducing SDS-PAGE, and gels were silver-stained (*A*) or transferred and probed on Western blots with polyclonal anti-GAA PAb2443 (*B*) or anti-IGF-II (*C*). Sizes of molecular mass markers (*lane M*) are labeled in kDa.

Tissues were homogenized using a rotor/stator homogenizer and then measured for glycogen content in a blinded format using the Amplex Red glucose assay kit (Invitrogen) essentially as described (14). For each tissue site, an analysis of variance was performed to obtain a pooled estimate of variance, and two-sided *t* tests within the analysis of variance model were performed to compare each pair of the five treatments, for a total of 10 comparisons. *p* values less than 0.05 are considered nominally statistically significant. GAA activity levels were measured in duplicate from the homogenized tissues, and the averages are reported as units/mg protein in Table 2.

## RESULTS

*GILT-GAA Has Enzymatic Activity Comparable with Untagged GAA*—Fig. 1 shows SDS-PAGE of rhGAA and GILT-tagged-GAA (BMN 701) purified from culture supernatants of transiently transfected suspension HEK293 cells. SDS-PAGE analysis shows that the purified rhGAA preparation is predominantly the 110,000-kDa full-length precursor and contains detectable amounts of the 95- and 75-kDa processed species. HEK293-produced BMN 701, which contains the GILT tag fused to position 70 of GAA, migrates with A slightly higher $M_r$ due to the presence of the GILT tag (Fig. 1*A*). Western blot analysis with anti-GAA antibodies (Fig. 1*B*) and an anti-IGF2 tag antibody (Fig. 1*C*) confirms the identity of the GAA polypeptide in both samples and the presence of the GILT tag in purified BMN 701.

The enzymatic activity of the two compounds was measured using a synthetic substrate, PNP α-glucoside. The specific activities of rhGAA and BMN 701 were 143,000 and 140,000 units/mg, respectively. Specific activities for CHO-produced BMN 701 ranged from 137,000 to 150,000 units/mg. Saturation

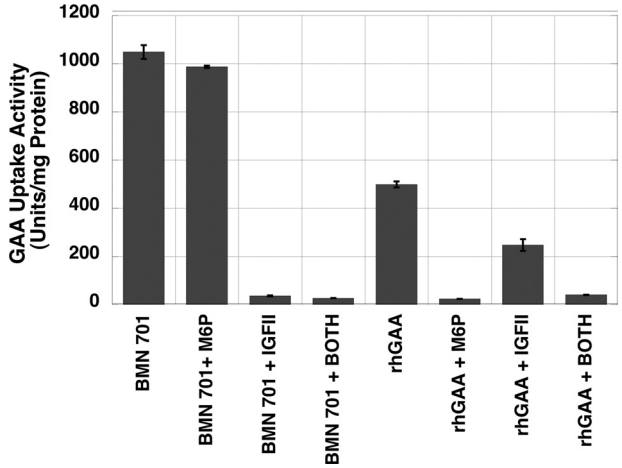


FIGURE 2. **Uptake of recombinant GAA in L6 rat myoblasts.** HEK293-produced BMN 701 and rhGAA were added at concentrations of 97 and 251 nM, respectively, to wells containing L6 cells. Inhibitors (5 mM M6P, 2.4 mM IGF-II, or both M6P and IGF-II) were also included in some wells. Uptake of the recombinant proteins is expressed as units of GAA activity/mg of cellular lysate. Each *data point* represents the average of duplicate samples. *Error bars* represent standard deviation.

curves yielded similar $K_m$ values of 5.8 and 5.9 mM for rhGAA and BMN 701, respectively.

*The GILT Tag Mediates Uptake of BMN 701 into Cultured Myoblasts*—Fig. 2 shows the ability of excess M6P or IGF-II to inhibit uptake of BMN 701 and rhGAA into rat L6 myoblasts. Cellular uptake of GILT-tagged BMN 701 is not inhibited by excess M6P but is inhibited completely by excess IGF-II. These data are consistent with the prediction that uptake of BMN 701 would occur by binding of the GILT tag to the IGF-II binding site of the CI-MPR. Uptake of rhGAA is inhibited completely by M6P, indicating that its internalization relies solely on M6P recognition by the M6P binding sites on the CI-MPR. Excess IGF-II partially competes for uptake of rhGAA. This phenomenon has been reported previously for other M6P-bearing lysosomal enzymes and has been attributed to steric hindrance of the M6P sites when IGF-II engages its cognate binding site on the receptor (31).

The specificity of the receptor-mediated uptake of the GILT-tagged BMN 701 protein was confirmed by uptake inhibition studies using two protein competitors derived from the CI-MPR (Fig. 3). Receptor construct 1288 contains domains 10–13 of the CI-MPR, sufficient to bind IGF-II but not M6P (32, 33). Receptor construct 1355 is identical to 1288 except for a single amino acid substitution that decreases its affinity for IGF-II (34). Neither receptor fragment inhibits uptake of rhGAA (Fig. 3*A*), indicating that rhGAA does not bind to the IGF-II binding domain of the CI-MPR. In contrast, construct 1288 is a potent inhibitor of BMN 701 uptake, and 1355 is a poor inhibitor (Fig. 3*B*). These data prove that uptake of BMN 701 occurs through interaction of the GILT tag with the IGF-II binding domain of the CI-MPR.

*Intracellular Processing of GILT-tagged and Untagged GAA Is Similar*—The kinetics of GAA enzyme activity decay after uptake of rhGAA and BMN 701 into L6 myoblasts were determined over a 14-day period (Fig. 4). The proteins have comparable half-lives of 8.3 and 9.0 days for rhGAA and BMN 701, respectively.

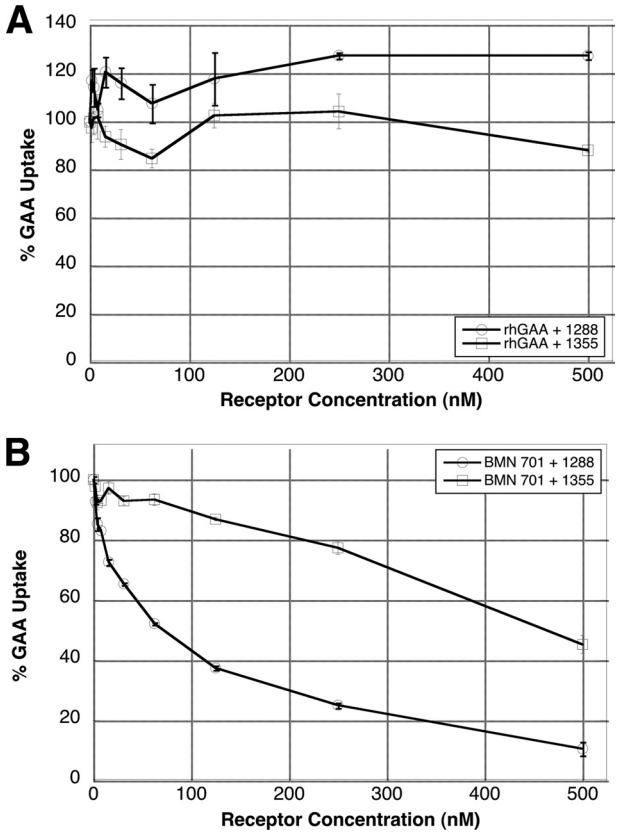


FIGURE 3. **Uptake inhibition of HEK293-produced BMN 701 by the IGF-II binding domain of the CI-MPR.** Uptake assays with 10 nM loadings of rhGAA (*A*) or HEK293-produced BMN 701 (*B*) were performed in the presence of increasing amounts (0–250 nM) of soluble receptor fragments 1288 (*circles*, wild-type IGF-II binding domain) or 1355 (*squares*, mutated IGF-II binding domain). Enzyme uptake is expressed as a percentage of the uptake in wells lacking receptor fragment inhibitors. Each *data point* represents the average of duplicate samples. *Error bars* represent standard deviation.

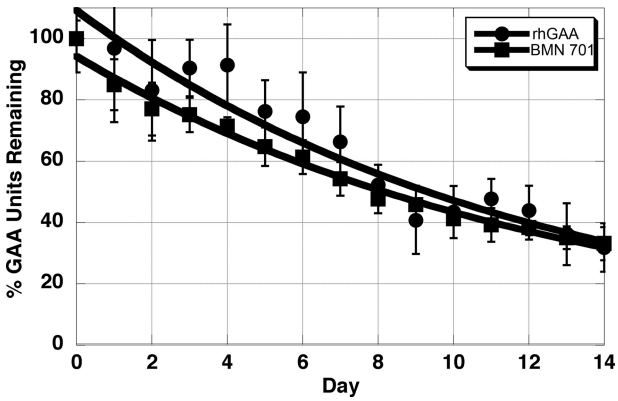


FIGURE 4. **Determination of the half-life of rhGAA and HEK293-produced BMN 701 within L6 cells.** Multiple wells with L6 cells were loaded with rhGAA (*circles*) at 235 nM or BMN 701 (*squares*) at 90 nM. Following an 18-h uptake incubation, all cells were washed four times with growth medium. Day 0 samples were then lysed and frozen, and the remaining samples were cultured for up to 14 days with triplicate wells harvested and frozen daily (*Days 1–14*). GAA units present in cell lysates are expressed as a percentage of activity of the Day 0 samples. *Error bars* display standard deviation. Data were fit to a first-order exponential decay curve using KaleidaGraph software to determine the enzymatic half-life. This experiment was repeated three times, and representative results are shown.

Once internalized, the 110-kDa precursor form of rhGAA is processed sequentially in the lysosome to an intermediate 95-kDa form, then to the mature 76- and 70-kDa forms. Smaller

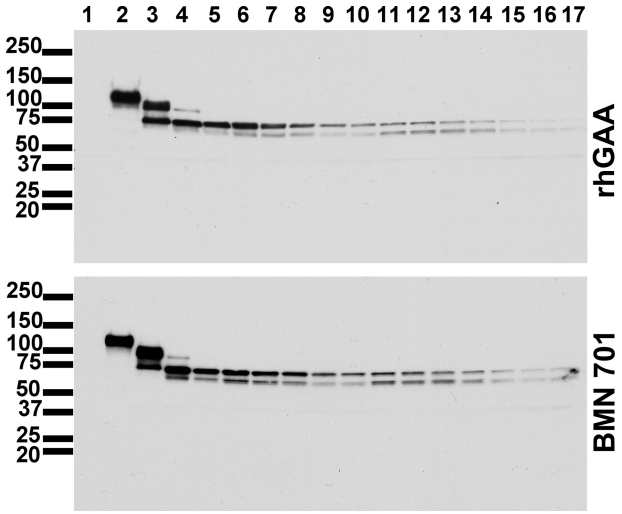


FIGURE 5. **Intracellular processing of rhGAA and HEK293-produced BMN 701.** Cell lysates from half-life uptake assays (Fig. 4) on rhGAA (*upper panel*) and BMN 701 (*lower panel*) were probed on Western blots with monoclonal antibody 3A6-1F2, which recognizes an epitope within amino acid residues 204–482 of human GAA. Sizes of molecular mass markers are labeled in kDa on the *left* of the panels. *Lane 1*, L6 lysate from cells grown in the absence of GAA protein; *lane 2*, rhGAA (*upper panel*) and FS701 (*lower panel*) uptake load material; *lanes 3–17*, L6 lysate harvested on days 0–14, respectively. This experiment was repeated three times, and representative results are shown.

peptide fragments released from the precursor form by proteolysis have been shown to remain associated with the 76- and 70-kDa fragments to form a multicomponent enzyme complex (35).

Western analysis of lysates from the time course reveal proteolytic processing of the full-length rhGAA and BMN 701 precursor proteins during the initial 18-h uptake (day 0) to predominantly the 95,000- and 75,000-kDa forms (Fig. 5). By day 2, the 75,000- and 70,000-kDa forms predominate and then slowly decay through day 14. Overall, the processing profiles of tagged and untagged GAA appear identical. The BMN 701 GILT tag is undetectable in lysates even at the earliest time point post-uptake as measured by Western blot using anti-tag antibody, suggesting that it is degraded immediately upon entering the lysosome (data not shown).

*Stable CHO Cell Production of GILT-tagged GAA*—To improve production of GILT-tagged GAA, a stable CHO cell line was generated using the coding region of the p701 DNA cassette and the GPEx® retrovector expression system (Catalent). Following multiple rounds of transfection and selection, the cell line sCHO-S-GAA 701-R35 was chosen for production of the CHO cell-derived protein designated BMN 701. Typical titers of BMN 701 from this system are ~250 mg/liter at scales up to 1000 liters. All of the measured biochemical properties of CHO-produced BMN 701 were found to be similar to those of HEK293-produced BMN 701, including mobility on SDS-PAGE, reactivity with anti-GAA and anti-GILT tag antibodies, $K_m$ and $V_{max}$ for the synthetic PNP substrate, uptake kinetics, and intracellular processing (data not shown).

*Internalized GILT-tagged GAA Is Delivered to the Lysosomes of C2C12 Myoblasts*—Although the intracellular processing of GILT-tagged GAA is consistent with a lysosomal localization of the protein, this was confirmed by demonstrating co-localization of BMN 701 with the lysosomal marker LAMP1. C2C12 mouse myoblasts were cultured in the presence and absence of GILT-tagged BMN 701. Fluorescently tagged antibodies against human GAA and mouse lysosomal marker LAMP1 (36) were then used to probe the cells (Fig. 6). Anti-GAA antibody detects internalized protein in cells cultured with BMN 701 but not in cells grown in the absence of BMN 701. The staining pattern of the anti-GAA antibody in individual cells grown with BMN 701 is indistinguishable from the staining pattern of anti-LAMP1, indicating that GILT-tagged BMN 701 is internalized and trafficked to the lysosome.

*GILT-tagged GAA Has Enhanced Delivery to Myoblasts Compared with Alglucosidase Alfa—In vitro* rat L6 myoblast cell uptake assays were performed with increasing amounts of BMN 701 to generate uptake saturation curves (Fig. 7). For comparison, uptake saturation curves were generated with untagged rhGAA, which was also used in animal testing, and with the currently approved Pompe enzyme replacement therapy, alglucosidase alfa, manufactured by Genzyme Corp., which was unavailable for animal testing. The cell uptake kinetics of HEK293-produced rhGAA and alglucosidase alfa are indistinguishable, with $K_{uptake}$ values of 141 and 147 nM, respectively. GILT-tagged BMN 701, however, shows a 26-fold enhancement in cellular delivery compared with alglucosidase alfa or rhGAA, with a $K_{uptake}$ value of 5.4 nM. Additionally, the BMN 701 uptake saturated reproducibly at a level ~2-fold greater than either of the untagged enzymes (1100 units/mg for BMN 701 compared with 619 and 516 units/mg for alglucosidase alfa and rhGAA, respectively).

*GILT-tagged GAA Has High Affinity for the CI-MPR*—To gauge the affinity of GILT-tagged BMN 701 for the IGF-II binding site on the CI-MPR, we compared its binding affinity with that of full-length recombinant IGF-II using surface plasmon resonance (Fig. 8). Association with the IGF-II binding domain (domains 10–13) of receptor fragment 1288 was measured using receptor 1355 (I1572T mutant) as a negative binding control. The $K_d$ values for the interaction of BMN 701 and IGF-II were determined by both a 1:1 Langmuir fit of the association and dissociation rate constants and by steady state kinetics (Table 1 and Fig. 8). The $K_d$ determined for the interaction of IGF-II with the domain 10–13 construct is 2.5 nM by Langmuir and 8.8 nM by steady state kinetics. The $K_d$ determined for interaction of BMN 701 with the domain 10–13 construct is 16 nM by Langmuir and 21 nM by steady state kinetics, within 6.4- and 2.4-fold, respectively, of the $K_d$ values determined for IGF-II. Linnell *et al.* (33) reported that IGF-II binds to a domain 10–13 construct with a $K_d$ 8.6-fold greater than for binding to domains 1–15 of the receptor, indicating that other domains of the receptor stabilize the interaction. If this ratio held for BMN 701, then the $K_d$ for binding to the intact receptor would be about 2 nM, a value that is in good agreement with the $K_{uptake}$ determined in uptake studies. Other literature values of the $K_d$ for IGF-II binding the complete CI-MPR range from 0.2 to 16 nM (37–39). Considering the tighter binding of IGF-II for the intact receptor, the determined $K_d$ value for IGF-II binding to the domain 10–13 construct is consistent with the lower end of this range. Binding of rhGAA to the domain 10–13 construct was not detected (data not shown).

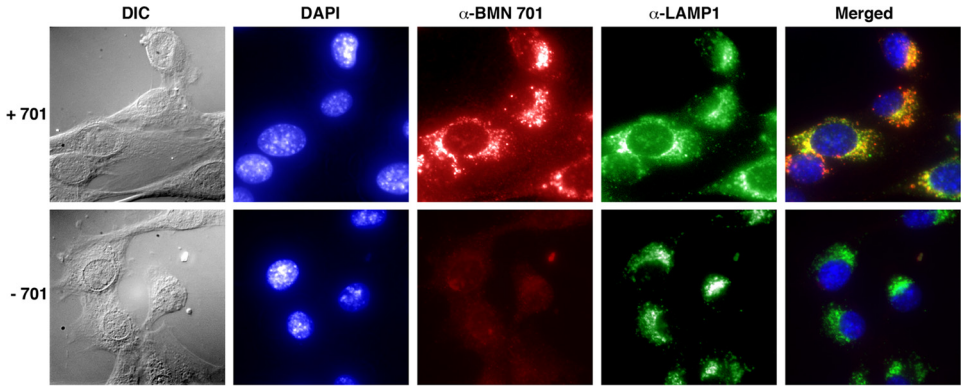


FIGURE 6. **Intracellular localization of CHO-produced BMN 701.** C2C12 cells grown in the presence (*upper images*) or absence (*lower images*) of BMN 701 were examined using immunofluorescence microscopy. Whole cells were imaged with differential interference contrast (*DIC*) filters. Nuclear DNA was imaged with a DAPI filter. CHO-produced BMN 701 was imaged with anti-human GAA primary antibody 3A6-1F2 (*α-BMN 701 panels*), anti-mouse IgG AF594 secondary antibody, and a Texas Red filter. Lysosomal LAMP1 was imaged with FITC-conjugated anti-LAMP1 primary antibody (*α-LAMP1 panels*) and a FITC filter. Fluorescent images were overlaid (*merged panels*).

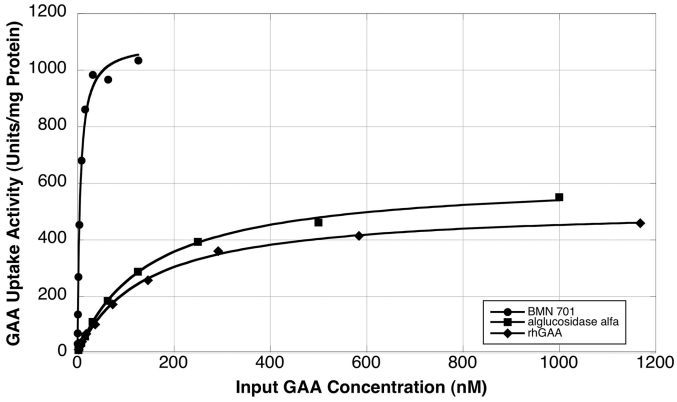


FIGURE 7. **Determination of *K*uptake for CHO-produced BMN 701, HEK293-produced rhGAA, and alglucosidase alfa.** Uptake assays with increasing amounts of GAA protein BMN 701 (*circles*), rhGAA (*squares*), or alglucosidase alfa (CHO-produced rhGAA manufactured by Genzyme) (*triangles*) were performed. Each point is the average of duplicate samples. Data points were fit to the Michaelis-Menten equation to determine $K_{uptake}$ values of 5.4, 141, and 147 nM for BMN 701, rhGAA, and alglucosidase alfa, respectively.

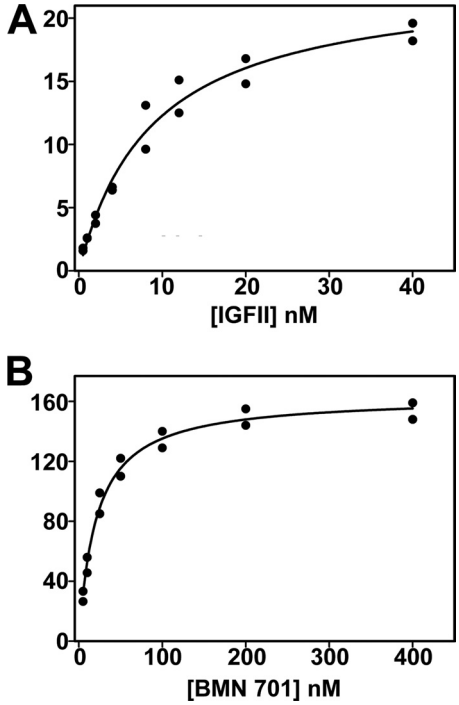


FIGURE 8. **Determination of affinity of BMN 701 for the IGF-II binding domain of the CI-MPR by surface plasmon resonance.** Similar amounts of the biotinylated CI-MPR constructs 1355 and 1288 were immobilized on the surface of a SA sensor chip (280 and 300 RU, respectively). IGF-II and BMN 701 were injected in a volume of 120 μl over the 1355 and 1288 coupled flow cells at a rate of 40 μl/min. After 2 min, the solutions containing the analyte were replaced with buffer, and the complexes were allowed to dissociate for 3 min. An average of the $R_{eq}$ values was determined for each analyte concentration using BIAevaluation version 4.0.1 software. Shown are equilibrium plots for IGF-II (0.5, 1, 2, 4, 8, 12, 20, and 40 nM) (*A*) and BMN 701 (5, 10, 25, 50, 100, 200, and 400 nM) (*B*). Equilibrium constants were calculated using nonlinear regression (SigmaPlot version 10.0) and are summarized in Table 1.

*GILT-tagged GAA Enhances Clearance of Glycogen from Mouse Muscle Tissue Compared with rhGAA*—The abilities of BMN 701 and rhGAA to reverse the storage pathology in Pompe mice was tested by administering the compounds to mice in a 4-week enzyme replacement protocol. The uptake kinetics of the HEK-produced rhGAA used in this experiment were evaluated as described above (Fig. 7).

Mice received four injections of BMN 701 or rhGAA at doses of either 5 or 20 mg/kg. The reduction in glycogen storage was greater in both dosing groups receiving BMN 701 compared with those receiving rhGAA (Fig. 9). In all tissues, treatment with the 20 mg/kg dose of BMN 701 resulted in statistically significant ($p < 0.05$) lower levels of glycogen than either the 20 or 5 mg/kg dose of rhGAA. Except for in the lingual musculature, treatment with 5 mg/kg BMN 701 resulted in significantly ($p < 0.05$) lower levels of glycogen than the 5 mg/kg dose of rhGAA. In the tibialis anterior, extensor digitorum longus, gastrocnemius, heart, and quadriceps, treatment with the 5 mg/kg dose of BMN 701 resulted in significantly ($p < 0.05$) lower levels of glycogen than treatment with 20 mg/kg rhGAA. No correlation was found between glycogen clearance and tissue GAA activity (Table 2). This is presumably because of the accumulation of significant quantities of GAA enzyme in capillary endothelial cells in muscle tissue (15).

## DISCUSSION

The rationale for enzyme replacement therapy for Pompe disease is that the underlying molecular cause of Pompe disease, accumulation of excess glycogen in the lysosomes of car-

**TABLE 1**
**Surface plasmon resonance analysis**

| Ligand | Langmuir 1:1 fit | | | | Steady-state kinetics | |
|---|---|---|---|---|---|---|
| | $k_a$ | $k_d$ | $K_d$ | $R_{max}$ | $K_d$ | $R_{max}$ |
| | *1/ms* | *1/s* | *nM* | *RU* | *nM* | *RU* |
| BMN 701 | $3.6 \times 10^5 \pm 1.9 \times 10^3$ | $5.8 \times 10^{-3} \pm 1.4 \times 10^{-5}$ | 16 | 146 | 21 ± 1.9 | 163 ± 3.7 |
| IGF-II | $1.1 \times 10^6 \pm 8.8 \times 10^3$ | $3.4 \times 10^{-3} \pm 2.8 \times 10^{-5}$ | 2.5 | 16.1 | 8.8 ± 1.2 | 23 ± 1.2 |

diac and skeletal muscle tissue due to insufficient amounts of GAA enzyme in the lysosome, can be reversed by delivery of sufficient GAA to the lysosomes of these cells. This should permit degradation of the accumulated lysosomal glycogen, reversal of the underlying cellular pathology, and improved clinical outcomes for patients.

In contrast to rhGAA, BMN 701 has a high affinity ligand for the CI-MPR on every enzyme molecule. Consequently, BMN 701 is taken up and delivered to the lysosome 26-fold more efficiently than is rhGAA, enabling BMN 701 to be about 5-fold more effective than rhGAA in its ability to clear glycogen from skeletal muscle of Pompe mice. These results demonstrate the validity of the hypothesis that increasing the affinity of GAA for the CI-MPR will lead to increased clearance of the glycogen stored in lysosomes of Pompe mice.

BMN 701 was designed to fulfill a number of criteria essential for an improved enzyme replacement therapy for Pompe disease. First, the presence of the GILT tag in BMN 701 must not interfere with the biological properties of GAA; next, the GILT tag GAA must enable high affinity binding of the BMN 701 molecule to the CI-MPR and subsequent trafficking to the lysosome; and finally, BMN 701 must improve clearance of glycogen from the lysosomes of heart and skeletal muscle. Initial attempts to fuse the GILT tag to the C terminus of GAA resulted in chimeras with enzymatically inactive GAA domains (data not shown). Moving the GILT tag to the N terminus of GAA, however, allowed proper function of both the GAA domain and the GILT tag. The GAA domain of GILT-tagged BMN 701 functions indistinguishably from rhGAA as measured by a number of criteria: enzymatic specific activity, $K_m$, $V_{max}$, intracellular half-life (Fig. 4), and intracellular processing (Fig. 5).

A variety of approaches was used to demonstrate that BMN 701 binds to the CI-MPR with high affinity and is routed to the lysosome. Surface plasmon resonance analysis (Table 1 and Fig. 8) is consistent with BMN 701 acting as a high affinity ligand for the receptor. This is borne out in *in vitro* cell uptake studies (Fig. 7), where $K_{uptake}$ values of GILT-tagged GAA are over 26-fold lower than untagged rhGAAs. Once bound to the receptor, BMN 701 appears to be trafficked to the lysosome as determined by immunofluorescence (Fig. 6). Specificity of GILT-tagged GAA uptake for the CI-MPR is demonstrated in competition experiments with both IGF-II (Fig. 2) and soluble receptor 1288 (Fig. 3). Uptake of GILT-tagged GAA produced in HEK293 cells (Fig. 2) and in CHO cells (data not shown) is not inhibited by excess M6P, indicating that uptake is almost completely dependent on the GILT tag. This suggests that the level of M6P on BMN 701 is considerably less than the levels present on the untagged rhGAA. This may be attributed to the different signal peptides used to express the two proteins. BMN 701 is expressed containing the IGF-II signal sequence, and rhGAA is expressed containing the native GAA signal sequence. Even though native GAA is poorly phosphorylated, replacement of the native signal sequence with that from IGF-II is likely to change the post-translational glycosylation. In fact substitution of the IGF-II signal peptide for the endogenous GAA signal peptide results in a GAA molecule with diminished M6P-dependent uptake, possibly because of alterations in the kinetics of GAA trafficking (data not shown). The native GAA signal peptide is reported to be inefficiently cleaved (40), which could extend its residence time in the Golgi, where M6P addition occurs.

Finally, BMN 701 is significantly more potent than untagged rhGAA in muscle tissue glycogen clearance in the Pompe mouse model (Fig. 9). In most muscle tissues examined, BMN 701 doses of 5 mg/kg led to greater clearance of glycogen than untagged rhGAA doses of 20 mg/kg. BMN 701 appears most effective in clearing glycogen from the heart, soleus, tibialis anterior, extensor digitorum longus, gastrocnemius, and quadricep. A sufficient amount of commercially available rhGAA (alglucosidase alfa) could not be obtained for this animal experiment, and thus, despite the fact that the uptake kinetics in rat L6 myoblasts of the rhGAA used in this study were virtually indistinguishable from those of alglucosidase alfa (Fig. 7), the possibility of other differences between the two untagged rhGAAs, such as differences in the sialic acid content of the glycan, limited the ability to draw conclusions about the relative performance of the two rhGAAs in animals.

Current enzyme replacement therapies for the treatment of lysosomal storage diseases rely on the binding of rhGAA to the CI-MPR via M6P moieties on the glycosylated rhGAA protein. The work presented here shows an alternative route for engagement of the receptor via an IGF-II-derived GILT tag fused to the rhGAA molecule. This alternative may hold several advantages over current enzyme replacement therapy for Pompe disease. For example, use of the GILT targeting strategy is compatible with non-mammalian expression systems that do not produce M6P-containing oligosaccharides on proteins. Also, because the glycosylation state of proteins can be variable and influenced by cell culture conditions, large scale production of enzymes that relies on specific glycosylation for their biological activity, such as M6P-dependent targeting, can face technical challenges. This appears to have been the case with alglucosidase alfa, where differences in pharmacokinetics and biodistribution between lots produced at the 160-liter scale and the 2000-liter scale were attributed to differences in glycosylation by the FDA, leading to the filing of a new biological license application for the 2000-liter-produced rhGAA (41).

Another potential advantage of BMN 701 relates to the observation that uptake of BMN 701 into rat L6 myoblasts sat-

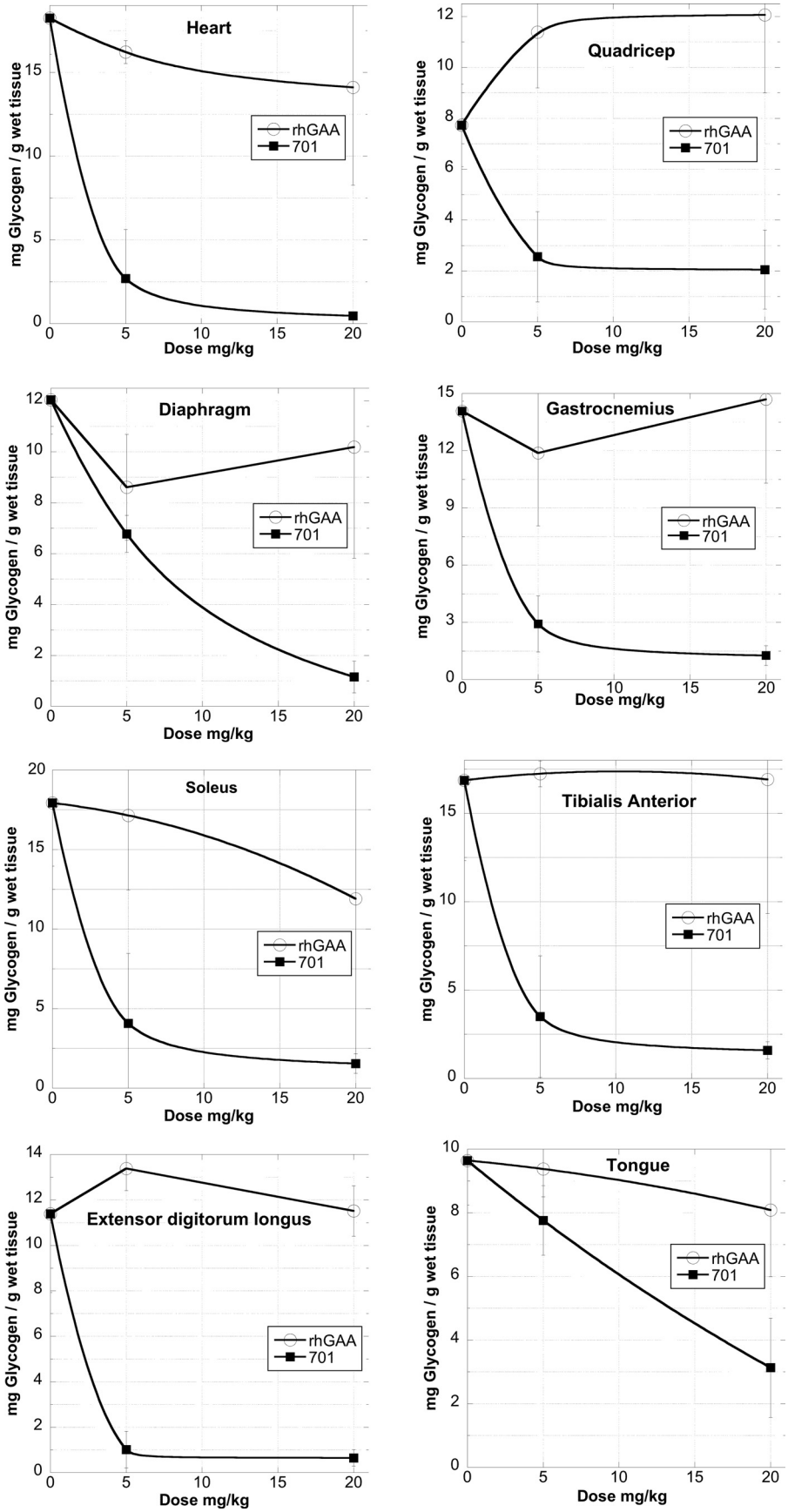


FIGURE 9. **Glycogen clearance in Pompe mice.** Glycogen levels were measured in various muscle tissues following four injections with CHO-produced BMN 701 or rhGAA. See "Experimental Procedures" for details.

**TABLE 2**
**Tissue GAA activity (units/mg protein) after 4 weekly treatments**

| Tissue | Treatment group | | | | |
|---|---|---|---|---|---|
| | PBS[a] | rhGAA | BMN 701 | rhGAA | BMN 701 |
| | | *5 mg/kg* | *5 mg/kg* | *20 mg/kg* | *20 mg/kg* |
| Heart | 3.9 ± 0.3 | 4.4 ± 0.7 | 6.3 ± 1.3 | 5.1 ± 2.1 | 5.4 ± 0.7 |
| Diaphragm | 5.3 ± 0.3 | 6.4 ± 1.1 | 7.8 ± 0.4 | 42 ± 54 | 25 ± 28 |
| Quadricep | 4.0 ± 0.3 | 4.4 ± 0.2 | 6.2 ± 1.1 | 9.2 ± 3.3 | 6.7 ± 1.4 |
| Soleus | 7.5 ± 3.1 | 7.3 ± 1.2 | 14 ± 2.8 | 34.4 ± 22 | 21 ± 6.7 |
| Gastrocnemius | 4.4 ± 0.2 | 4.8 ± 0.3 | 7.3 ± 0.9 | 16 ± 9.7 | 7.5 ± 1.4 |
| EDL[b] | 6.7 ± 1.2 | 7.2 ± 0.5 | 9.1 ± 0.8 | 24 ± 13 | 13 ± 1.9 |
| TA[c] | 4.8 ± 0.8 | 4.7 ± 0.1 | 7.4 ± 0.5 | 20 ± 13 | 7.1 ± 1.3 |
| Tongue | 4.6 ± 0.5 | 4.8 ± 0.5 | 4.8 ± 0.3 | 10.5 ± 3.9 | 5.7 ± 0.5 |
| Liver | 7.3 ± 1.8 | 61 ± 15 | 47 ± 4.3 | 187 ± 17 | 184 ± 17 |

[a] Vehicle.
[b] EDL, extensor digitorum longus.
[c] TA, tibialis anterior.

urates at approximately twice the level at which rhGAA uptake saturates. This observation could be explained by postulating that the IGF-II tag on BMN 701 binds to the IGF-I receptor and triggers redistribution of the CI-MPR to the plasma membrane. IGF-I, IGF-II, and insulin have all been shown to promote redistribution of the CI-MPR to the cell surface (16, 17). The IGF-II stimulatory effect was shown to be sensitive to the phosphatidylinositol 3-kinase (PI3K) inhibitor, wortmannin (18), suggesting that CI-MPR redistribution is triggered by binding of IGF-II to the IGF-I receptor, a receptor known to activate PI3K (23). We do not know whether the concentration of BMN 701 at the surface of a muscle fiber after intravenous injection would be sufficient to trigger this signaling pathway, but experiments to test this hypothesis are under way.

*Acknowledgments—The BIAcore 3000 instrument was purchased through a grant from the Advancing a Healthier Wisconsin program. The 129-GAA$^{-/-}$ Pompe mouse line used in these experiments was derived from the original strain kindly provided by Nina Raben. We thank Denise Cloutier for expert technical assistance with in vivo studies and Dr. Richard M. Bittman for statistical analysis. We also acknowledge the many thoughtful comments on the manuscript from colleagues at BioMarin.*

## REFERENCES

1. Hers, H. G. (1963) α-Glucosidase deficiency in generalized glycogenstorage disease (Pompe's disease) *Biochem. J.* **86,** 11–16
2. Lejeune, N., Thines-Sempoux, D., and Hers, H. G. (1963) Tissue fractionation studies. 16. Intracellular distribution and properties of α-glucosidases in rat liver. *Biochem. J.* **86,** 16–21
3. Hirschhorn, R., and Reuser, A. (2001) Glycogen storage disease type II: acid α-glucosidase (acid maltase) deficiency, in *The Metabolic and Molecular Basis of Inherited Disease* (Scriver, C. R., Beaudet, A. L., Sly, W. S., and Valle, D., eds), 8th Ed., pp. 3389–3420, McGraw-Hill, New York
4. Brown, B. I., Brown, D. H., and Jeffrey, P. L. (1970) Simultaneous absence of α-1,4-glucosidase and α-1,6-glucosidase activities (pH 4) in tissues of children with type II glycogen storage disease. *Biochemistry* **9,** 1423–1428
5. Reuser, A. J., Kroos, M. A., Hermans, M. M., Bijvoet, A. G., Verbeet, M. P., Van Diggelen, O. P., Kleijer, W. J., and Van der Ploeg, A. T. (1995) Glycogenosis type II (acid maltase deficiency). *Muscle Nerve* supplement **3,** S61–S69
6. Kishnani, P. S., Hwu, W. L., Mandel, H., Nicolino, M., Yong, F., and Corzo, D. (2006) A retrospective, multinational, multicenter study on the natural history of infantile-onset Pompe disease. *J. Pediatr.* **148,** 671–676
7. Winkel, L. P., Hagemans, M. L., van Doorn, P. A., Loonen, M. C., Hop, W. J., Reuser, A. J., and van der Ploeg, A. T. (2005) The natural course of non-classic Pompe's disease; a review of 225 published cases. *J. Neurol.* **252,** 875–884
8. Amalfitano, A., Bengur, A. R., Morse, R. P., Majure, J. M., Case, L. E., Veerling, D. L., Mackey, J., Kishnani, P., Smith, W., McVie-Wylie, A., Sullivan, J. A., Hoganson, G. E., Phillips, J. A., 3rd, Schaefer, G. B., Charrow, J., Ware, R. E., Bossen, E. H., and Chen, Y. T. (2001) Recombinant human acid α-glucosidase enzyme therapy for infantile glycogen storage disease type II: results of a phase I/II clinical trial. *Genet. Med.* **3,** 132–138
9. Kishnani, P. S., Corzo, D., Nicolino, M., Byrne, B., Mandel, H., Hwu, W. L., Leslie, N., Levine, J., Spencer, C., McDonald, M., Li, J., Dumontier, J., Halberthal, M., Chien, Y. H., Hopkin, R., Vijayaraghavan, S., Gruskin, D., Bartholomew, D., van der Ploeg, A., Clancy, J. P., Parini, R., Morin, G., Beck, M., De la Gastine, G. S., Jokic, M., Thurberg, B., Richards, S., Bali, D., Davison, M., Worden, M. A., Chen, Y. T., and Wraith, J. E. (2007) Recombinant human acid α-glucosidase: major clinical benefits in infantile-onset Pompe disease. *Neurology* **68,** 99–109
10. van der Ploeg, A. T., Clemens, P. R., Corzo, D., Escolar, D. M., Florence, J., Groeneveld, G. J., Herson, S., Kishnani, P. S., Laforet, P., Lake, S. L., Lange, D. J., Leshner, R. T., Mayhew, J. E., Morgan, C., Nozaki, K., Park, D. J., Pestronk, A., Rosenbloom, B., Skrinar, A., van Capelle, C. I., van der Beek, N. A., Wasserstein, M., and Zivkovic, S. A. (2010) A randomized study of alglucosidase alfa in late-onset Pompe's disease. *N. Engl. J. Med.* **362,** 1396–1406
11. Nicolino, M., Byrne, B., Wraith, J. E., Leslie, N., Mandel, H., Freyer, D. R., Arnold, G. L., Pivnick, E. K., Ottinger, C. J., Robinson, P. H., Loo, J. C., Smitka, M., Jardine, P., Tatò, L., Chabrol, B., McCandless, S., Kimura, S., Mehta, L., Bali, D., Skrinar, A., Morgan, C., Rangachari, L., Corzo, D., and Kishnani, P. S. (2009) Clinical outcomes after long-term treatment with alglucosidase alfa in infants and children with advanced Pompe disease. *Genet. Med.* **11,** 210–219
12. Raben, N., Nagaraju, K., Lee, E., Kessler, P., Byrne, B., Lee, L., LaMarca, M., King, C., Ward, J., Sauer, B., and Plotz, P. (1998) Targeted disruption of the acid α-glucosidase gene in mice causes an illness with critical features of both infantile and adult human glycogen storage disease type II. *J. Biol. Chem.* **273,** 19086–19092
13. Raben, N., Danon, M., Gilbert, A. L., Dwivedi, S., Collins, B., Thurberg, B. L., Mattaliano, R. J., Nagaraju, K., and Plotz, P. H. (2003) Enzyme replacement therapy in the mouse model of Pompe disease. *Mol. Genet. Metab.* **80,** 159–169
14. Zhu, Y., Li, X., McVie-Wylie, A., Jiang, C., Thurberg, B. L., Raben, N., Mattaliano, R. J., and Cheng, S. H. (2005) Carbohydrate-remodelled acid α-glucosidase with higher affinity for the cation-independent mannose 6-phosphate receptor demonstrates improved delivery to muscles of Pompe mice. *Biochem. J.* **389,** 619–628
15. McVie-Wylie, A. J., Lee, K. L., Qiu, H., Jin, X., Do, H., Gotschall, R., Thurberg, B. L., Rogers, C., Raben, N., O'Callaghan, M., Canfield, W., Andrews, L., McPherson, J. M., and Mattaliano, R. J. (2008) Biochemical and pharmacological characterization of different recombinant acid α-glucosidase preparations evaluated for the treatment of Pompe disease. *Mol. Genet. Metab.* **94,** 448–455
16. Braulke, T., Tippmer, S., Neher, E., and von Figura, K. (1989) Regulation of the mannose 6-phosphate/IGF II receptor expression at the cell surface by mannose 6-phosphate, insulin-like growth factors, and epidermal growth factor. *EMBO J.* **8,** 681–686
17. Villevalois-Cam, L., Tahiri, K., Chauvet, G., and Desbuquois, B. (2000) Insulin-induced redistribution of the insulin-like growth factor II/mannose 6-phosphate receptor in intact rat liver. *J. Cell. Biochem.* **77,** 310–322
18. Körner, C., and Braulke, T. (1996) Inhibition of IGF II-induced redistribution of mannose 6-phosphate receptors by the phosphatidylinositol 3-kinase inhibitor, wortmannin. *Mol. Cell. Endocrinol.* **118,** 201–205
19. Fukuda, T., Ewan, L., Bauer, M., Mattaliano, R. J., Zaal, K., Ralston, E., Plotz, P. H., and Raben, N. (2006) Dysfunction of endocytic and autophagic pathways in a lysosomal storage disease. *Ann. Neurol.* **59,** 700–708
20. Raben, N., Fukuda, T., Gilbert, A. L., de Jong, D., Thurberg, B. L., Mattaliano, R. J., Meikle, P., Hopwood, J. J., Nagashima, K., Nagaraju, K., and Plotz, P. H. (2005) Replacing acid α-glucosidase in Pompe disease: recombinant and transgenic enzymes are equipotent, but neither completely

clears glycogen from type II muscle fibers. *Mol. Ther.* **11,** 48–56
21. Van der Ploeg, A. T., Kroos, M. A., Willemsen, R., Brons, N. H., and Reuser, A. J. (1991) Intravenous administration of phosphorylated acid α-glucosidase leads to uptake of enzyme in heart and skeletal muscle of mice. *J. Clin. Invest.* **87,** 513–518
22. Yang, H. W., Kikuchi, T., Hagiwara, Y., Mizutani, M., Chen, Y. T., and Van Hove, J. L. (1998) Recombinant human acid α-glucosidase corrects acid α-glucosidase-deficient human fibroblasts, quail fibroblasts, and quail myoblasts. *Pediatr. Res.* **43,** 374–380
23. Myers, M. G., Jr., Grammer, T. C., Wang, L. M., Sun, X. J., Pierce, J. H., Blenis, J., and White, M. F. (1994) Insulin receptor substrate-1 mediates phosphatidylinositol 3′-kinase and p70S6k signaling during insulin, insulin-like growth factor-1, and interleukin-4 stimulation. *J. Biol. Chem.* **269,** 28783–28789
24. Tong, P. Y., and Kornfeld, S. (1989) Ligand interactions of the cation-dependent mannose 6-phosphate receptor. Comparison with the cation-independent mannose 6-phosphate receptor *J. Biol. Chem.* **264,** 7970–7975
25. Zhu, Y., Jiang, J. L., Gumlaw, N. K., Zhang, J., Bercury, S. D., Ziegler, R. J., Lee, K., Kudo, M., Canfield, W. M., Edmunds, T., Jiang, C., Mattaliano, R. J., and Cheng, S. H. (2009) Glycoengineered acid α-glucosidase with improved efficacy at correcting the metabolic aberrations and motor function deficits in a mouse model of Pompe disease. *Mol. Ther.* **17,** 954–963
26. LeBowitz, J. H., Grubb, J. H., Maga, J. A., Schmiel, D. H., Vogler, C., and Sly, W. S. (2004) Glycosylation-independent targeting enhances enzyme delivery to lysosomes and decreases storage in mucopolysaccharidosis type VII mice. *Proc. Natl. Acad. Sci. U.S.A.* **101,** 3083–3088
27. Bremel, R. D., Miller, L. U., and Bleck, G. T. (2005) Host cells containing multiple integrating vectors. U. S. Patent 6852510
28. Oshima, A., Nolan, C. M., Kyle, J. W., Grubb, J. H., and Sly, W. S. (1988) The human cation-independent mannose 6-phosphate receptor. Cloning and sequence of the full-length cDNA and expression of functional receptor in COS cells. *J. Biol. Chem.* **263,** 2553–2562
29. Blum, H., Beier, H., and Gross, H. J. (1987) Improved silver staining of plant proteins, RNA, and DNA in polyacrylamide gels. *Electrophoresis* **8,** 93–99
30. Myszka, D. G. (2000) Kinetic, equilibrium, and thermodynamic analysis of macromolecular interactions with BIACORE. *Methods Enzymol.* **323,** 325–340
31. Kiess, W., Thomas, C. L., Greenstein, L. A., Lee, L., Sklar, M. M., Rechler, M. M., Sahagian, G. G., and Nissley, S. P. (1989) Insulin-like growth factor-II (IGF-II) inhibits both the cellular uptake of β-galactosidase and the binding of β-galactosidase to purified IGF-II/mannose 6-phosphate receptor. *J. Biol. Chem.* **264,** 4710–4714
32. Dahms, N. M., and Hancock, M. K. (2002) P-type lectins. *Biochim. Biophys. Acta* **1572,** 317–340
33. Linnell, J., Groeger, G., and Hassan, A. B. (2001) Real time kinetics of Insulin-like growth factor II (IGF-II) interaction with the IGF-II/mannose 6-phosphate receptor. The effects of domain 13 and pH. *J. Biol. Chem.* **276,** 23986–23991
34. Garmroudi, F., Devi, G., Slentz, D. H., Schaffer, B. S., and MacDonald, R. G. (1996) Truncated forms of the insulin-like growth factor II (IGF-II)/mannose 6-phosphate receptor encompassing the IGF-II binding site: characterization of a point mutation that abolishes IGF-II binding. *Mol. Endocrinol.* **10,** 642–651
35. Moreland, R. J., Jin, X., Zhang, X. K., Decker, R. W., Albee, K. L., Lee, K. L., Cauthron, R. D., Brewer, K., Edmunds, T., and Canfield, W. M. (2005) Lysosomal acid α-glucosidase consists of four different peptides processed from a single chain precursor. *J. Biol. Chem.* **280,** 6780–6791
36. Chen, J. W., Pan, W., D'Souza, M. P., and August, J. T. (1985) Lysosome-associated membrane proteins: characterization of LAMP-1 of macrophage P388 and mouse embryo 3T3 cultured cells. *Arch. Biochem. Biophys.* **239,** 574–586
37. Schmidt, B., Kiecke-Siemsen, C., Waheed, A., Braulke, T., and von Figura, K. (1995) Localization of the insulin-like growth factor II binding site to amino acids 1508–1566 in repeat 11 of the mannose 6-phosphate/insulin-like growth factor II receptor. *J. Biol. Chem.* **270,** 14975–14982
38. Tong, P. Y., Tollefsen, S. E., and Kornfeld, S. (1988) The cation-independent mannose 6-phosphate receptor binds insulin-like growth factor II. *J. Biol. Chem.* **263,** 2585–2588
39. Valenzano, K. J., Heath-Monnig, E., Tollefsen, S. E., Lake, M., and Lobel, P. (1997) Biophysical and biological properties of naturally occurring high molecular weight insulin-like growth factor II variants. *J. Biol. Chem.* **272,** 4804–4813
40. Wisselaar, H. A., Kroos, M. A., Hermans, M. M., van Beeumen, J., and Reuser, A. J. (1993) Structural and functional changes of lysosomal acid α-glucosidase during intracellular transport and maturation. *J. Biol. Chem.* **268,** 2223–2231
41. Mack, G. (2008) FDA balks at Myozyme scale-up. *Nat. Biotechnol.* **26,** 592